PHYSICAL REVIEW E **84**, 041707 (2011)

Nematic-nematic phase transition in the liquid crystal dimer CBC9CB and its mixtures with 5CB: A high-resolution adiabatic scanning calorimetric study

Chandra Shekhar Pati Tripathi, Patricia Losada-Pérez, and Christ Glorieux
Laboratorium voor Akoestiek en Thermische Fysica, Departement Natuurkunde en Sterrenkunde, Katholieke Universiteit Leuven, Celestijnenlaan 200D, B-3001 Leuven, Belgium

Alexandra Kohlmeier, Maria-Gabriela Tamba, and Georg H. Mehl
Department of Chemistry, The University of Hull, Cottingham Road, Hull HU6 7RX, United Kingdom

Jan Leys[*]
Laboratorium voor Akoestiek en Thermische Fysica, Departement Natuurkunde en Sterrenkunde, Katholieke Universiteit Leuven, Celestijnenlaan 200D, B-3001 Leuven, Belgium

(Received 19 May 2011; revised manuscript received 19 September 2011; published 28 October 2011)

The phase transition behavior of the liquid crystal dimer α,ω-bis(4,4$'$-cyanobiphenyl)nonane (CBC9CB), which has been reported to exhibit a nematic-nematic phase transition, has been investigated by means of high-resolution adiabatic scanning calorimetry. This nematic-nematic phase transition is weakly first-order with a latent heat of 0.24 ± 0.01 kJ kg^{-1}. Mixtures up to 40 wt % with 4-pentyl-4$'$-cyanobiphenyl (5CB) liquid crystals have also been investigated, which also show this nematic to nematic phase transition. The transition stays weakly first-order with a decreasing latent heat with increasing concentration of 5CB. For mixtures with more than 40 wt % uniaxial nematic-unknown nematic phase transition was not observed.

DOI: 10.1103/PhysRevE.84.041707 PACS number(s): 42.70.Df, 65.40.Ba, 07.20.Fw, 64.70.M−

I. INTRODUCTION

Mesomorphic phase behavior of calamitic mesogens is characterized by the formation of one or more liquid crystal phases, formed on cooling from the isotropic state. The liquid crystalline phases are defined by different symmetries and low temperature phases are usually of lower symmetry and higher ordering than high temperature phases. Often phase sequences such as nematic-smectic (SmA, SmC, etc.)-crystalline are detected. The observation of more than one nematic phase is thus very unusual and hence multiple nematic phases and their phase transitions have over the years attracted considerable interest, ranging from theoretical efforts to experimental studies and the synthesis of new molecules [1]. This is due to the importance of understanding the formation of multiple nematic phases, moreover, it is anticipated to shed light on the features responsible for the formation of the biaxial nematic phase.

Initially the focus of research centered on re-entrant nematics, where two nematic phases, usually separated by a smectic phase, can be detected on varying the temperature [2,3]. This phase behavior is typically found for molecules with strong polar groups, where on cooling due to antiparallel correlations in a type of supramolecular organization entities with incommensurate length scales are formed. This destabilizes the smectic order and favors the formation of a nematic phase at a lower temperature.

This concept of supramolecular assembly in a liquid crystal matrix where the assembled structure in turn controls the organization of the liquid crystal phase is very powerful. It can be extended to other molecular architectures, such as the formation of a columnar nematic phase (N_{Col}) at temperatures below a discotic nematic phase (N_D) [4] or in polymers with discotic nematic groups, the formation of a nematic lamellar phase (N_L) due to assembly formation has been described [5].

Higher levels of supramolecular organization with decreasing temperature can be attributed to the formation of different levels of organization and this has been used to explain successfully nematic-cybotactic nematic phase sequences in bent-core mesogens [6]. For these systems the proximity to the formation of the biaxial nematic phase is noteworthy.

For liquid crystal main chain polymers experimental and theoretical effort has shown that a thermotropic phase sequence with two adjacent uniaxial nematic phases can occur [7,8]. Theory suggests that, depending on the length and flexibility of alkyl chains connecting mesogenic groups, the formation of two uniaxial nematic phases is possible [9], however, temperature dependent folding and unfolding of the liquid crystal polymer has been considered as well [10].

Mesogenic groups linked by flexible spacers, usually termed dimers and often treated as model systems for polymeric and dendrimeric liquid crystals [11], have been investigated in considerable detail to study the odd-even effects of hydrocarbon groups on the liquid crystal phase stability and the correlations between chemical structure and the formation of nematic and smectic phases [12,13].

For most of these materials, odd spaced systems have much lower transition temperatures than the even membered series, a feature attributed to differences in the molecular conformations of even membered molecules with an essentially fully extended, almost linear structure and bent conformations of odd membered systems. Most extensively studied have been the α,ω-bis(4-cyanobiphenyl-4$'$-yloxy)alkanes [13–15]. At lower temperatures such systems either form a smectic phase (e.g., SmA) or crystallize directly.

---

[*] Researcher for Research Foundation–Flanders (FWO); jan.leys@fys.kuleuven.be

The introduction of a disulfide bridge in the center of the flexible methylene spacer has been reported to induce an as yet unidentified second uniaxial nematic phase [16]. A similar effect has been detected in dimers consisting of some salicyladimine based mesogens with odd spacers [17] and some bentcore-calamitic dimers [18].

Quite surprisingly uniaxial nematic-nematic transitions have been detected by some of us in a set of dimers of quite different structures, where the common feature is a direct link of the hydrocarbon chain to the aromatic groups of the mesogenic moieties [19,20]. This phase behavior is in contrast to the phase behavior of the alkoxy variants discussed above. For a heptyl spaced dimer containing two cyanobiphenyl groups there has been some controversy in the assignment of the liquid crystal (LC) phase behavior [21–23]. For a nonyl hydrocarbon chain a "hairpin" or "bent" conformation has been observed in the crystalline state [24]. For the undecyl spaced compound the existence of two nematic phases has been confirmed by x-ray diffraction and optical investigations [19].

The observed phase sequence from uniaxial nematic to unknown nematic phase (N_u-N_x) in the cyanobiphenyl dimers possibly suggests that the mesogens can change conformation between extended and bent. The former corresponds to the terminal mesogenic dipole moments being antiparallel to each other and hence zero net longitudinal dipole moment, while in the latter case the dipoles are parallel to each other so that the system possesses a net dipole moment [23]. The conformational nature of the N_u-N_x phase transition is supported by a more recent statistical-mechanical study by Photinos and co-workers, in which a substantial probability of bent-shaped conformation was observed for the odd spacer cyanobiphenyl dimers [25].

Quite surprisingly very little research focus has centered on the clear classification of the phase transitions of dimeric liquid crystals, and none so far where two nematic phases have been detected. Considering the importance of this question, the astonishing simplicity of the structures and their chemical proximity to the archetypal nematic system 4-pentyl-4$'$-cyanobiphenyl (5CB), this is in our view a question that needs to be addressed. Thus we have carried out a systematic high-resolution adiabatic scanning calorimetry study on the phase sequence of the pure compound α,ω-bis(4,4$'$-cyanobiphenyl)nonane (CBC9CB) in order to unambiguously determine the order and energy content of this uniaxial nematic to unknown nematic phase transition (N_u-N_x).

From macroscopic thermodynamic specific heat capacity and enthalpy data it is obviously not possible to determine the type of the phases studied. To do this one has to rely on methods [like x-ray diffraction (XRD)] probing the molecular arrangements of the phases considered. For the compound CBC9CB and for the mixtures with 5CB such information is indeed presented in Ref. [20] showing both phases to be nematic (see also further in Sec. II). Unambiguously determining the order of the N_u-N_x transition, as can be done by adiabatic scanning calorimetry (ASC), will produce important information on the symmetry of the two phases. Indeed, if the symmetries are the same the transition will be first-order. Different symmetries can result in transitions that are first-order or second-order or tricritical (where a first-order crosses over to a second-order one). The nematic to isotropic transition is known to be weakly first-order and close to a tricritical point. Whether there are similarities for the N_u-N_x and whether it is (weakly) first-order, second-order, or exhibits tricriticallity can be deduced from high-resolution specific heat capacity and enthalpy data near the transition.

II. MATERIALS AND METHODS

CBC9CB is a liquid crystal dimer with polar cyanobiphenyl groups in the end separated by an alkyl chain of nine carbon atoms. It was synthesized in the Department of Chemistry at the University of Hull (United Kingdom). Its chemical structure and phase sequence are shown in Fig. 1. Upon cooling from the isotropic phase it exhibits a uniaxial nematic phase and the above mentioned unknown nematic phase prior to crystallization. The liquid crystal 5CB was supplied by Merck. Several mixtures of CBC9CB with 5CB were prepared, namely $x = 5$, 12.5, 25, 30, 35, 40, where x stands for the wt % of 5CB in the mixtures.

As already referred to above, XRD evidence for the existence of two different nematic phases was presented in [20] for the pure CBC9CB compound. Evidence from XRD for the mixtures with 5CB was also reported in Ref. [20]. That these two phases observed in CBC9CB are indeed nematic can be verified from the XRD results displayed in Fig. 2(a) for the N_u phase and in Fig. 2(b) for the N_x phase. Detailed reporting on the x-ray work (already partly reported in Ref. [20]) in the mixtures with 5CB and other compounds will be done in a forthcoming paper.

High-resolution adiabatic scanning calorimetry (ASC) was employed for a thorough investigation exploring the phase behavior of the pure compound as well as the mixtures prepared with the 5CB liquid crystal. Both heating and cooling runs were performed for the pure compound as well as for the mixtures. The ASC setup used was fully automated via LABVIEW (National Instruments) software and consisted of four stages. The inner stage was a 10-g molybdenum cell, which was surrounded by three outer shields. The cell also contains a stirring ball made of stainless steel. An automatic mechanism changes the inclination of the whole apparatus and so the ball moves back and forth in order to eliminate any temperature gradients within the sample and to maintain the homogeneity in the mixture. A vacuum pump was used to evacuate the surrounding space between the cell and the three shields down to 10^{-6} mbar to reduce the thermal coupling among the different stages and to ensure thermal insulation. The heat capacity of the empty cell was measured in a separate calibration experiment. It was then subtracted from the total

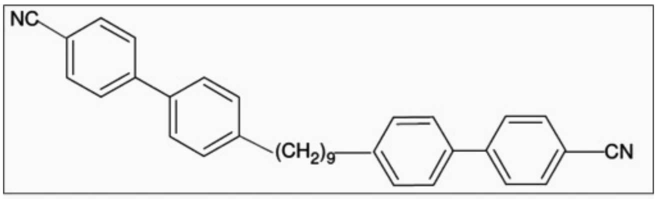

Cr 356.60 K $\mathbf{N_x}$ 377.59 K $\mathbf{N_u}$ 392.92 K **Iso**

FIG. 1. The chemical structure, the phase sequence, and the transition temperatures (obtained by ASC) of the CBC9CB compound.

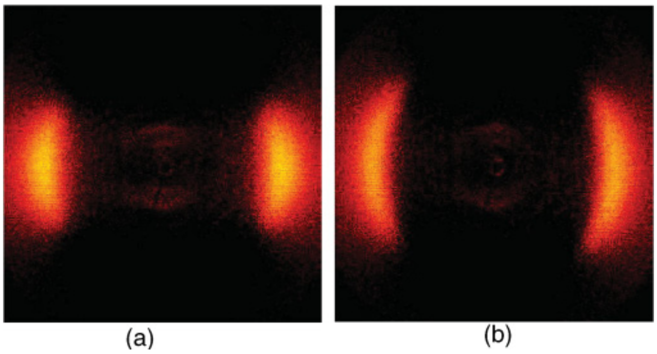

FIG. 2. (Color online) (a) CBC9CB in the magnetic field on cooling: XRD patterns of the nematic N_u phase at 393.15 K: the intensity of the isotropic liquid is subtracted. (b) XRD patterns of low temperature N_x phase of aligned samples of compound CBC9CB in the magnetic field on cooling: XRD patterns of the nematic N_x at 373.15 K: the intensity of the isotropic liquid is subtracted. The diffractograms show typical features of a nematic phase: a diffuse wide angle scattering located around the equator, dominating the XRD pattern and a diffuselike scattering on the meridian in the small angle region. The position and the intensity of the small angle scattering change only slightly going from the N_u to the N_x phase.

heat capacity (which is the sum of the cell and the sample) and then divided by the mass of the sample in order to derive the specific heat capacity of the sample.

In adiabatic scanning calorimetry very slow scanning rates down to 0.5 mK per minute can be achieved, thus ensuring the thermodynamic equilibrium of the sample. In order to obtain the temperature dependence of the heat capacity $C_p(T)$ and the enthalpy $H(T)$ a constant power P is supplied to the sample and the resulting change in temperature $T(t)$ is measured as a function of time t. From P and $T(t)$, the heat capacity can easily be obtained as follows:

$$C_p = \frac{P}{\dot{T}(t)}, \tag{1}$$

with $\dot{T}(t) = dT/dt$ the time derivative of the temperature, to be calculated numerically. The exact knowledge of $T(t)$ allows also the direct calculation of the enthalpy $H(T)$ as a function of temperature by inverting the $T(t)$ data to

$$H(T) = H(T_s) + P[t(T) - t_s(T_s)], \tag{2}$$

with T_s the starting temperature of the run at t_s. The continuous determination of the enthalpy as a function of temperature provides a unique tool for determining the order of a phase transition. In the principal modes of operation (continuous heating or cooling) of ASC, a constant heating or cooling power is applied so the temperature change rate slows down substantially in the coexistence region since the power is dissipated not only for the temperature change of the sample but also for the enthalpy change between the two coexisting phases. This allows an exact determination of the two phase region and the latent heat in a first-order phase transition. A more detailed description of ASC can be found elsewhere [26–28].

III. RESULTS AND DISCUSSION

In this section we present the results obtained from ASC runs for the pure compound (Sec. III A) as well as for the mixtures of the pure compound with 5CB liquid crystal (Sec. III B).

A. Pure CBC9CB

Several heating and cooling runs have been performed for the pure compound CBC9CB. A description of the runs, including the temperature range and the average scanning rate, is given in Table I.

In Fig. 3 the isotropic-uniaxial nematic (I-N_u) and the uniaxial nematic-unknown nematic (N_u-N_x) transitions corresponding to the slowest (run 2) heating run are shown for CBC9CB. The temperature dependent heat capacity $C_p(T)$ for both transitions is plotted in Fig. 3(a) and the temperature dependent enthalpy $H(T)$ is shown in Fig. 3(b).

Subsequent heating and cooling runs revealed that the I-N_u transition takes place at $T_{IU} = 392.92$ K, which is lower than the transition temperature obtained from a differential scanning calorimetry (DSC) thermogram ($T_{IU} = 395.90$ K) [20]. This difference in the phase transition temperature has most likely to do with the different purity of the sample, as the compound that we investigated in this work was from a different batch than the one investigated via DSC studies. However, the transition peak in the ASC data is rather sharp so apparently the possible differences in purity of the sample affect only the transition temperature. For ASC data we define the I-N_u transition temperature T_{IU} as the temperature where the system starts losing its orientational order, i.e., the temperature where the heat capacity values start to evolve abruptly in a heating run. The phase transition is weakly first-order with a latent heat of $L_{IU} = 1.2 \pm 0.1$ kJ kg^{-1}. The heat capacity exhibited the usual pretransitional behavior below and above the transition as observed in other systems [29]. The two-phase region is clearly visible and extends over 120 ± 10 mK.

A very sharp first-order phase transition is observed for the conventional nematic to the low temperature nematic phase (N_u-N_x). The uniaxial nematic to unknown nematic phase transition is also weakly first-order with a latent heat of $L_{UX} = 0.24 \pm 0.01$ kJ kg^{-1} and a two phase region of 80 ± 10 mK. The N_u-N_x phase transition temperature is $T_{UX} = 377.22$ K, which both for the pure compound as well for the mixtures with 5CB is again slightly lower than that obtained in earlier DSC

TABLE I. Measurement parameters of runs performed on pure CBC9CB.

Run	Type of run	T range (K)	Scanning rate[a] (K h^{-1})
1	heating	360-400	0.50
2	heating	374-395	0.15
3	cooling	398-365	0.60
4	cooling	375-395	0.25

[a] Scanning rate refers to the average rate, since in the phase-coexistence region the rate slows down.

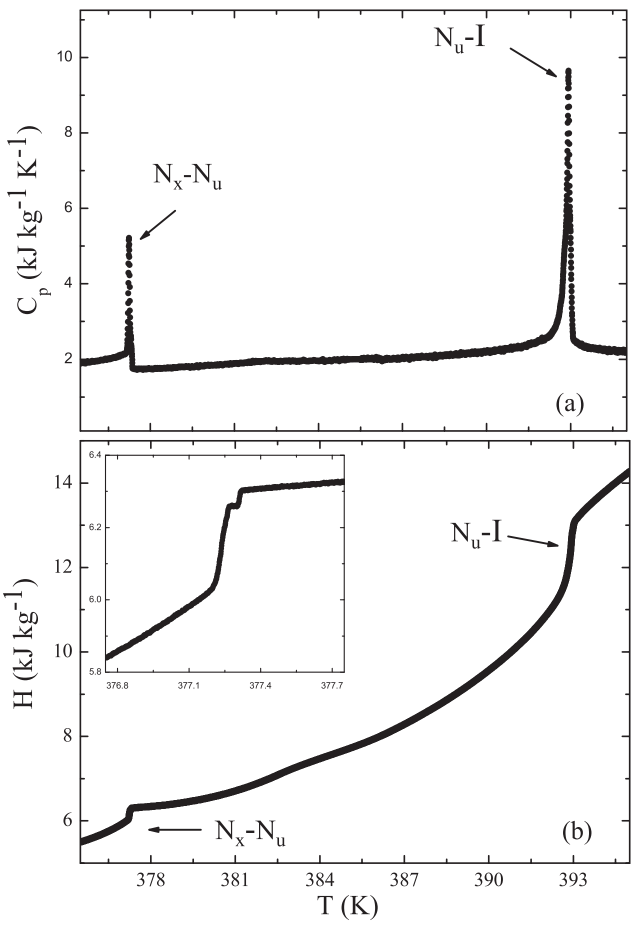

FIG. 3. (a) Temperature dependence of the specific heat capacity and (b) enthalpy curves for the N_u-N_x and I-N_u phase transitions, a blowup of the 1-K area around the N_u-N_x transition temperature as inset in the enthalpy diagram. The data plotted here correspond to the slowest heating run. A slow scanning rate of 0.15 K h^{-1} was used.

measurements ($T_{UX} = 380.45$ K). The heat capacity shows a pretransitional increase in the lower temperature nematic phase. The transition temperatures between different heating and cooling runs were almost the same and the slight hysteresis that was observed is typical for first-order phase transitions.

B. Mixtures of CBC9CB with 5CB

In addition to the pure compound, various mixtures with 5CB have also been studied by ASC. The N_u-N_x phase transition was observed up to 40 wt % of 5CB in the mixtures, while in earlier reports this transition was seen up to 60 wt % of 5CB [20]. ASC measurements at higher concentrations turned out to be unreliable because of resolution limits, the low temperature limits (at room temperature) of the instrument, and possible supercooling. The phase transition temperatures for both N_u-N_x and I-N_u obtained via ASC together with the ones from DSC measurements as a function of increasing wt % of 5CB are plotted in Fig. 4. The temperature range of the uniaxial nematic phase (N_u) gets broadened with increasing concentration of 5CB.

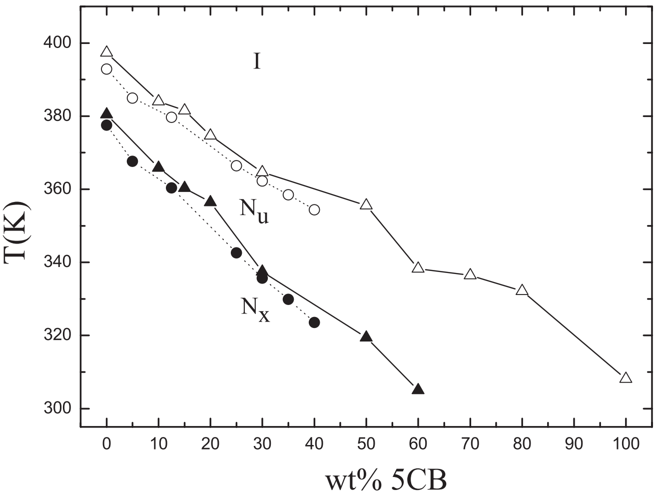

FIG. 4. The I-N_u (open symbols) and N_u-N_x (closed symbols) phase transition temperatures of the pure CBC9CB compound and mixtures with 5CB investigated by ASC (open and closed circles) and DSC (open and closed triangles) [20] as a function of wt % of 5CB. The solid and dotted lines through the symbols are included as a guide to the eye.

From a detailed study of the $C_p(T)$ and $H(T)$ curves near the N_u-N_x phase transition, the ASC transition temperatures, latent heat values, and the phase coexistence range for the N_u-N_x phase transition for the pure compound and for the mixtures with 5CB are given in Table II. The latent heat values L_{UX} are plotted as a function of the wt % of 5CB in the mixtures in Fig. 5. The latent heat for the transition from the lower temperature nematic phase to the higher temperature nematic phase decreases with increasing wt % of 5CB down to very small values. This reduction is stronger than the one that could be expected on the basis of the corresponding reduction of CBC9CB per unit mass.

In Figs. 6 and 7 the heat capacity $C_p(T)$ profiles are shown for the heating runs of all the mixtures with 5CB as a function of T-T_{UX} where T_{UX} is defined as the temperature where the heat capacity values starts to evolve abruptly in a heating run. The data sets are plotted on the same temperature scale in order to compare the effect of various concentrations of 5CB in the mixtures. When increasing the concentration of 5CB, the N_x-N_u transition is shifted to a lower temperature and the heat capacity peak is reduced.

TABLE II. Characteristics of the N_u-N_x phase transition for pure CBC9CB and the mixtures with 5CB.

wt % of 5CB	T_{UX} (K)	ΔT_{coex} (mK)	L_{UX} (kJ kg^{-1})
0.0	377.22	80 ± 10	0.24 ± 0.01
5.0	367.70	72 ± 8	0.14 ± 0.01
12.5	360.43	60 ± 5	0.10 ± 0.01
25.0	342.65	55 ± 5	0.040 ± 0.002
30.0	335.70	40 ± 4	0.0195 ± 0.002
35.0	329.92	35 ± 5	0.011 ± 0.003
40.0	323.62	20 ± 4	0.0062 ± 0.0004

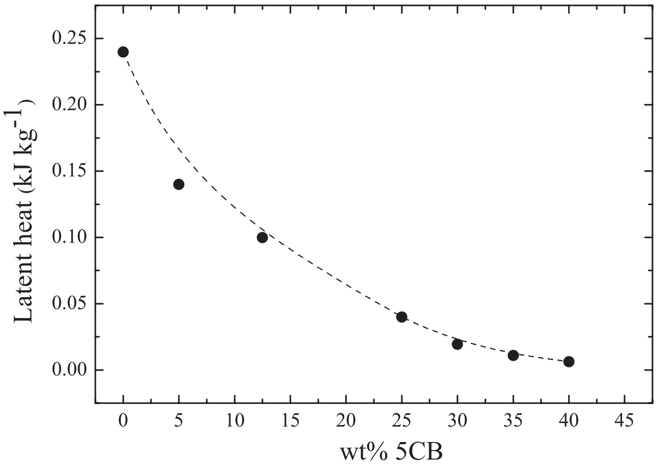

FIG. 5. The latent heat values of the N_u-N_x phase transition for the pure compound and all the mixtures as a function of wt % of 5CB. The dashed line is a quadratic fit through the symbols. The error on the measurements is about 5–10% (see Table II).

This behavior may be attributed to the influence on the competition effect between the two possible configurations mentioned in the Introduction: the extended configuration (antiparallel orientation of the mesogenic units) and the bent configuration (parallel orientation of the mesogenic units). We can conclude that the presence of 5CB reinforces the stability of the uniaxial nematic phase N_u thus precluding that of the N_x phase.

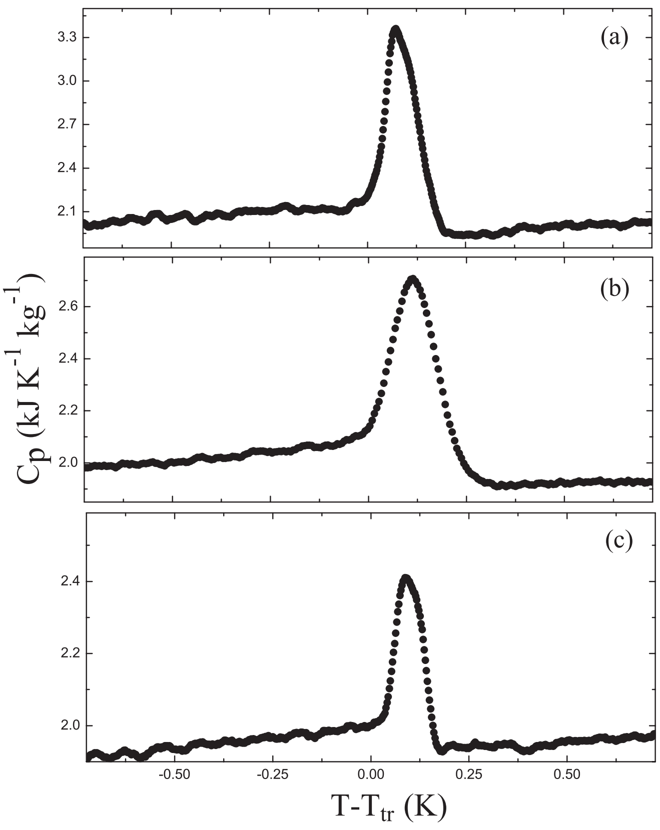

FIG. 6. The heat capacity profiles of the heating runs performed on the mixtures of CBC9CB and 5CB: (a) 5 wt %, (b) 12.5 wt %, and (c) 25 wt % of 5CB for N_u-N_x phase transition.

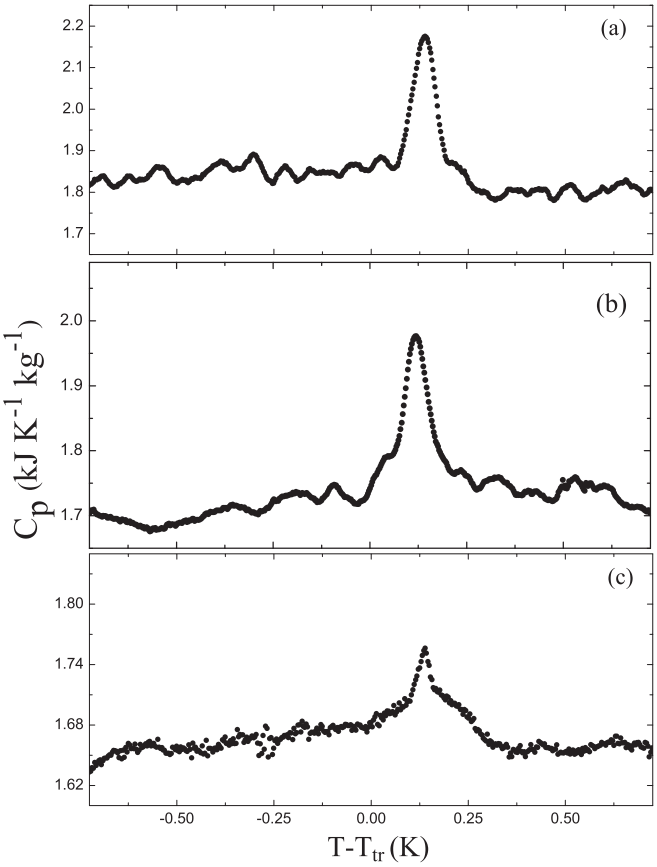

FIG. 7. The heat capacity profiles of the heating runs performed on the mixtures of CBC9CB and 5CB: (a) 30 wt %, (b) 35 wt %, and (c) 40 wt % of 5CB for N_u-N_x phase transition.

IV. ANALYSIS OF THE PRETRANSITIONAL HEAT CAPACITIES

As reported in Sec. III A, the N-I and N_u-N_x phase transitions in the pure compound are both weakly first-order. The pretransitional increase on the low temperature side of the transition in the specific heat capacity is a characteristic of this type of phase transition, which can be described by the following power law [30]:

$$C_p(T) = A_0\left(\frac{T^{**}-T}{T^{**}}\right)^{-\alpha} + B + E\left(\frac{T^{**}-T}{T^{**}}\right), \qquad (3)$$

where A_0 is the amplitude of the fluctuation induced pretransitional effect, T^{**} is the effective critical temperature, which is different than the first-order transition temperature T_{IU} at the N-I phase transition and T_{UX} at the N_u-N_x phase transition, B and E represent a constant and linear background term, respectively. The experimental data for the low temperature side both at the N-I and N_u-N_x phase transitions have been fitted to Eq. (3). The fit values for the uniaxial nematic phase at the N-I phase transition are shown in Table III. In fits 1 and 2, α was kept free and both yield an effective exponent smaller than 0.50 (tricritical mean field value [30]). Within the fitting

TABLE III. Parameter values from fits with the Eq. (3) for the uniaxial nematic phase at the N-I phase transition. Parameters in square brackets have been kept fixed to the indicated values.

Fit	A_0 (J kg^{-1} K^{-1})	α	T^{**} (K)	B (J kg^{-1} K^{-1})	E (J kg^{-1} K^{-1})	χ_ν^2
1	113.9	0.36	392.94	1385	0.3	1.08
2	102.6	0.37	392.95	141	[0]	1.10
3	34	[0.50]	392.95	1677	[0]	1.25

range (1.5 K) the inclusion of the linear term hardly changes the quality of the fit. A somewhat poorer fit was obtained when α was fixed at 0.50 (fit 3). These fitting results are in line with what is normally observed for N-I transitions in other types of compounds [29,30].

Since the N_u-N_x transition is a novel type of transition, more extensive fitting with the same expression (3) was performed for the pretransitional specific heat capacity in the unknown nematic phase at the N_u-N_x phase transition. The results for the pure compound and three different mixtures, with 5%, 12.5%, and 25% of 5CB, are reported in Table IV (for the very small anomalies of higher 5CB concentrations reliable fits could not be obtained).

Fits 1 and 2 shows that the linear background term is small, and fixing the parameter E to 0 has practically no influence on the fit quality. This was also verified for the other data sets and thus E was fixed to 0 for all other fits, for which range shrinking fits (T range from 3, 2, and 1 K) were performed as well. For the pure compound (fits 2–7) α was kept as a free parameter and fixed to 0.5. With α free, values around 0.37 are found, somewhat different from the tricritical value of 0.50. An expected correlation between the critical amplitude A_0 and exponent α is observed, however, as for the N-I transition fixing α to 0.5 hardly changes the quality of the fit. For the mixtures, in view of the small influence on the fit quality, α has been fixed to 0.50, and only these fits are reported in Table IV.

TABLE V. Latent heat of N_u-N_x phase transition, critical amplitude A_0 for the N_x phase and the ratio R between them for the pure compound as well as some of the mixtures with 5CB.

wt % of 5CB	L (J kg^{-1})	A_0 (J kg^{-1} K^{-1})	R (K)
0.0	240 ± 10	25.0 ± 3	10 ± 1
5.0	140 ± 10	13.0 ± 2	11 ± 2
12.5	100 ± 10	8.5 ± 1	12 ± 2
25.0	40 ± 2	0.1 ± 0.02	–

Fits 8–15 of Table IV are concerned with fitting of the data for the mixtures with 5%, 12.5%, and 25% of 5CB, respectively. Range shrinking fits verify the stability of the fits indicating that the used Eq. (3) provides a good description of the data in all cases. Thus from the data in Table IV, it can be seen that the pretransitional heat capacity of the N_u-N_x transition can be described by the standard expression for this quantity. More specifically, the results are consistent with a critical exponent reflecting tricritical behavior, or at least one that is close to the value $\alpha = 0.50$.

As can be seen from a comparison of Figs. 3, 6, and 7 there is a strong decrease of the specific heat capacity anomaly with increasing 5CB concentration. This should obviously be reflected in the amplitude of the singular term in Eq. (3). This decrease can best be quantified by comparing in Table IV the fit values for A_0 obtained at the fixed α value of 0.5, where a substantial decrease of A_0 can be noticed. In Table V the A_0 values for the different systems are compared with the corresponding latent heats. From the ratio of both quantities, within experimental uncertainty, a nearly constant ratio of 10 is obtained. From the fitting it follows that the N_u-N_x transition of the pure compound is close to a tricritical point, but it seems that the presence of 5CB does mainly results in a dilution effect and does not (observably) drive the system to or away from the tricritical point.

TABLE IV. Parameter values from fits with Eq. (3) for the unknown nematic phase at the N_u-N_x phase transition for the pure compound and some of the mixtures with 5CB. Parameters in square brackets have been kept fixed to the indicated values.

Fit	wt % of 5CB	$\Delta\tau$ range (K)	A_0 (J kg^{-1} K^{-1})	α	T^{**} (K)	B (J kg^{-1} K^{-1})	E (J kg^{-1} K^{-1})	χ_ν^2
1	0.0	3	67.8	0.36	377.63	1384.41	−0.0193	2.03
2	0.0	3	69.1	0.35	377.61	1434.7	[0]	2.02
3	0.0	3	25.5	[0.50]	377.75	1384.41	[0]	2.02
4	0.0	2	63.1	0.37	377.59	1451.21	[0]	2.17
5	0.0	2	24.8	[0.50]	377.68	1556.18	[0]	2.18
6	0.0	1	39.8	0.40	377.48	1384.41	[0]	2.34
7	0.0	1	18.2	[0.50]	377.52	1625.21	[0]	2.32
8	5.0	3	12.9	[0.50]	368.95	1325.00	[0]	1.64
9	5.0	2	13.3	[0.50]	368.01	1579.98	[0]	1.72
10	5.0	1	14.3	[0.50]	368.10	1573.61	[0]	1.80
11	12.5	3	7.9	[0.50]	362.92	1384.41	[0]	2.20
12	12.5	2	8.6	[0.50]	361.79	1384.41	[0]	2.22
13	12.5	1	8.8	[0.50]	362.05	1384.41	[0]	2.23
14	25.0	2	0.07	[0.50]	348.38	1032.4	[0]	2.01
15	25.0	1	0.08	[0.50]	348.36	1057.5	[0]	2.01

V. CONCLUSIONS

This paper presents a detailed investigation of the phase transition behavior of the liquid crystal cyanobiphenyl dimer CBC9CB and its mixtures with the liquid crystal 5CB by means of high-resolution adiabatic scanning calorimetry. Upon cooling from the isotropic phase the pure compound CBC9CB shows a uniaxial nematic phase and an unknown nematic phase prior to crystallization. Both the transitions from isotropic to uniaxial nematic and uniaxial nematic to unknown nematic are weakly first-order with latent heats of 1.2 ± 0.1 kJ kg^{-1} and 0.24 ± 0.01 kJ kg^{-1}, respectively. Mixtures with 5CB up to 40 wt % exhibit the same phase sequence. The transition from the uniaxial nematic to the unknown nematic phase stays first-order with a decreasing latent heat with increasing concentration of 5CB in the mixtures and was not observed for 5CB concentrations above 40 wt %.

The pretransitional increase of the specific heat capacity in the uniaxial nematic phase below the N-I transition has been analyzed in the framework of the mean field approximation expression of Eq. (3) yields an critical exponent α around 0.36 somewhat less than the tricritical value of 0.5, which also gives an acceptable fit. A similar analysis with Eq. (3) of the pretransitional specific heat capacity increase in the N_x phase below the N_u-N_x phase transition was carried out for both the pure component and the mixtures with 5CB added. In all cases critical exponent values around 0.5 are found. From a comparison between the latent heat of the N_u-N_x transition and the amplitude of the singular contribution of the specific heat capacity anomaly as a function of the concentration of 5CB an almost constant proportionality factor is found, indicating that the presence of 5CB in the mixtures mainly results in a dilution effect and does not drive the system closer to or away from the tricritical point.

ACKNOWLEDGMENTS

This research was supported by the Research Foundation–Flanders (FWO) Project "AVISCO" No. G.0230.07 and Project No. 1.5.125.10N. J.L. acknowledges FWO. C.S.P.T. is grateful to the K.U.Leuven Research Council for financial support. G.H.M. acknowledges the support through the E.U. Project "BIND."

[1] P. G. de Gennes and J. Prost, *The Physics of Liquid Crystals* (Oxford University Press, Oxford, 1993).
[2] P. E. Cladis, Mol. Cryst. Liq. Cryst. **165**, 85 (1988).
[3] P. E. Cladis, Liq. Cryst. **24**, 15 (1998).
[4] H. Ringsdorf, R. Wüstefeld, R. Zerta, M. Ebert, and J. H. Wendorff, Angew. Chem. Int. Ed. **28**, 914 (1989).
[5] P. H. J. Kouwer, W. F. Jager, W. J. Mijs, and S. J. Picken, Macromolecules **34**, 7582 (2001).
[6] C. Keith, A. Lehmann, U. Baumeister, M. Prehm, and C. Tschierske, Soft Matter **6**, 1704 (2010).
[7] G. Ungar, V. Percec, and M. Zuber, Macromolecules **25**, 75 (1992).
[8] G. Ungar, V. Percec, and M. Zuber, Polym. Bull. **32**, 325 (1994).
[9] S. V. Vasilenko, A. R. Khokhlov, and V. P. Shibaev, Macromolecules **17**, 2270 (1984).
[10] V. Percec, A. D. Asandei, and G. Ungar, Chem. Mater. **8**, 1550 (1996).
[11] A. G. Vanakaras and D. J. Photinos, J. Mater. Chem. **15**, 2002 (2005).
[12] C. T. Imrie and G. R. Luckhurst, *Handbook of Liquid Crystals, Vol. 2B: Low Molecular Weight Liquid Crystals II* (Wiley-VCH, Weinheim, 1998), pp 801–833.
[13] C. T. Imrie and P. A. Henderson, Chem Soc. Rev. **36**, 2096 (2007).
[14] J. W. Emsley, G. R. Luckhurst, G. N. Shilstone, and I. Sage, Mol. Cryst. Liq. Cryst. Lett. **102**, 223 (1984).
[15] G. R. Luckhurst, Liq. Cryst. **32**, 1335 (2005).
[16] B. Kundu, S. K. Pal, S. Kumar, R. Pratibha, and N. V. Madhusudana, Europhys. Lett. **85**, 36002 (2009).
[17] M. Šepelj, A. Lesac, U. Baumeister, S. Diele, D. W. Bruce, and Z. Hameršak, Chem. Mater. **18**, 2050 (2006).
[18] M.-G. Tamba, U. Baumeister, G. Pelzl, and W. Weissflog, Liq. Cryst. **37**, 853 (2010).
[19] V. P. Panov, M. Nagaraj, J. K. Vij, Yu. P. Panarin, A. Kohlmeier, M.-G. Tamba, R. A. Lewis, and G. H. Mehl, Phys. Rev. Lett. **105**, 167801 (2010).
[20] M.-G. Tamba, A. Kohlmeier, and G. H. Mehl, P3.57; 23rd International Liquid Crystal Conference, Kraków, Poland, 2010.
[21] P. J. Barnes, A. G. Douglass, S. K. Heeks, and G. R. Luckhurst, Liq. Cryst. **13**, 603 (1993).
[22] H. Toriumi, D. J. Photinos, and E. T. Samulski, First Pacific Polymer Conference Preprints **1**, 185 (1989).
[23] M. Cestari *et al.* 062; 23rd International Liquid Crystal Conference Kraków, Poland, 2010.
[24] K. Hori, M. Iimuro, A. Nakao, and H. Toriumi, J. Mol. Struct. **699**, 23 (2004).
[25] A. Kumar, P. K. Karahaliou, A. G. Vanakaras, and D. J. Photinos, P3.05; 11th European Conference on Liquid Crystals, Maribor, Slovenia, 2011.
[26] J. Thoen, H. Marynissen, and W. Van Dael, Phys. Rev. A **26**, 2886 (1982).
[27] J. Thoen, G. Cordoyiannis, and C. Glorieux, Liq. Cryst. **36**, 669 (2009).
[28] J. Thoen, *Heat Capacities: Liquids, Solutions and Vapours* (The Royal Society of Chemistry, London, 2010), pp. 287–306.
[29] B. Van Roie, J. Leys, K. Denolf, C. Glorieux, G. Pitsi, and J. Thoen, Phys. Rev. E **72**, 041702 (2005).
[30] M. A. Anisimov, *Critical Phenomena in Liquids and Liquid Crystals* (Gordon and Breach, New York, 1991).